Seasonal and interannual variability in absorbing aerosols over India derived from TOMS: Relationship to regional meteorology and emissions

Gazala Habib[1], Chandra Venkataraman[1], Isabelle Chiapello[2], S. Ramachandran[3], Olivier Boucher[2], M. Shekar Reddy[2]

[1]Department of Chemical Engineering, Indian Institute of Technology Bombay, Powai, Mumbai-400 076, India.
Department of Chemical Engineering, Indian Institute of Technology Bombay, Powai, Mumbai-400 076, India.
[2]Laboratoire d'Optique Atmospherique, UFR de Physique, Bat P5, Universite de Lille, Villeneuve d'Ascq Cedex, 59655, France.
[3]Space and Atmospheric Sciences Division, Physical Research Laboratory, Navrangpura, Ahmedabad 380 009, India.

Abstract

The objective of this study is an analysis of the spatial, seasonal and interannual variability of regional-scale aerosol load over India, detected by TOMS during 1981-2000, with an evaluation of potential contributing factors, including estimated anthropogenic aerosol emission trends and regional meteorology (rainfall and circulation patterns). The quality of the positively constrained TOMS aerosol index (TOMS Ai) over India, in terms of correlation with ground-based AOD data at four sites, was found to be satisfactory on a monthly time scale, and good on a daily time scale. Difficulties in obtaining conformity in averaging times and the presence of chemically mixed aerosols complicated the comparison at several other sites. Spatial distributions in TOMS Ai were related to the emission densities of anthropogenic absorbing aerosols in Apr-May, but varied seasonally and were modified significantly by higher atmospheric dispersion in Jan-Mar and rainfall in Jun-Sep, both of which lead to low TOMS Ai, even in regions of high aerosol emissions. The magnitude of TOMS Ai bore good to moderate relation to the anthropogenic aerosol emission flux in five selected regions, dominated by biomass/biofuel burning and fossil fuel combustion, but showed poor relationship region with large desert dust load. Absorbing aerosols in the biomass burning regions included black carbon (BC) and inorganic matter (IOM), while the latter, from coal fly-ash, dominated fossil fuel regions. The seasonal cycle in TOMS Ai was related to the seasonal variability in dust or open burning emissions and to rainfall. A link between regional circulation anomalies and those in the aerosol load detected by TOMS, was suggested by significant downward air-mass velocities, estimated in the NCEP reanalysis data, in years of high TOMS Ai compared to those of low TOMS Ai, extending over the entire northern part of the sub-continent covering the east, Indo-Gangetic plain, west and northwest, potentially leading to low atmospheric dispersion and high aerosol load. In several years, high TOMS Ai correlated with a decrease in SW monsoon rainfall in the south, west and northwest, while low TOMS Ai correlated with an increase in SW monsoon rainfall in the northeast, east and south. This relation is however only illustrative, because of the small data set analyzed here. Interannual variability in TOMS Ai was linked to that in forest burning emissions in the northeast, as evidenced by a correlation with ATSR fire-counts, both significantly enhanced in 1999. Increase in anthropogenic aerosol emissions from India during 1981-2000, especially 9-10% yr^{-1} from fossil fuel use, are significant in explaining trends in aerosol loading detected by TOMS over most regions of India.

1. Introduction

Large uncertainties are associated with the prediction of climate effects of aerosols [*Boucher and Haywood*; 2001; *Anderson et al.*, 2003], arising in part from their high temporal and spatial variability. Variability in aerosol loading over tropical India has been recorded through observational networks. For example, long-term measurements, made using a network of multi-wavelength radiometers, showed increases of 2-9% yr^{-1} in columnar aerosol optical depth at 400 nm, at locations like Thiruvananthapuram (8.5°N, 76.9°E; coastal), Vishakapatnam (17.7°N, 83.2°E; industrialized) and Mysore (12.3° N, 76.5°E; continental) during 1986-1998 [*Moorthy et al.*, 1999; *Moorthy,* 2001]. Upper tropospheric aerosol extinction coefficients, derived from balloon-borne sun scanning/tracking photometers at Hyderabad (17.5°N, 78.6°E) [*Ramachandran and Jayaraman*, 2003], increased by about 11±1% yr^{-1} during 1985-2001. Extensive aerosol optical and chemical measurements during the Indian Ocean Experiment (INDOEX) [*Ramanathan et al.*, 2001] showed significant concentrations of absorbing aerosols and associated optical depth during the NE monsoon (Jan-Mar), along with a large interannual variability in these parameters [*Moorthy et al.*, 2001; *Li and Ramanathan*, 2002; *Ramachandran and Jayaraman*, 2002]. Analysis of optical depth measurements at Kaashidhoo (Maldives, 4.9°N, 73.5°E), from AERONET, and Minicoy (8.3°N, 73.1°E), from radiometer measurements, in the near-IR at 1020 nm, indicated that dust aerosols, transported from NW India, and the Arabian and Saharan regions, dominate the optical depth during April-May [*Satheesh and Srinivasan*, 2002].

Here it is our interest to undertake an analysis of the spatial, seasonal and interannual variability of aerosol load over India on a regional-scale with an analysis of potential contributing factors. Satellite remote sensing has been successfully applied in deducing the origin, temporal and spatial distribution of absorbing aerosols [*Herman et al*., 1997; *Torres et al*., 1998; *Chiapello et al.*, 1999], and in constraining biomass-burning emissions [*Duncan et al.*, 2003]. The AVHRR (Advanced Very High-Resolution Radiometer) aerosol data set provides information on aerosol optical depth limited, however, to water surfaces [*Wen and Rose* 1994; *Husar et al.*, 1997]. The positively constrained spectral contrast in the ultra-violet range derived from TOMS (Total Ozone Mapping Spectrometer), termed TOMS Ai (TOMS aerosol index), has been successfully used to detect absorbing aerosols (i.e. desert mineral dust and smoke aerosol from biomass burning) in the UV range, both on land and ocean [*Hsu et al.*, 1996; *Herman et al.*, 1997; *Chiapello et al.*, 1999; *Duncan et al.*, 2003]. Correlations were found between TOMS Ai and sun photometer aerosol optical depth measurement for regions like Saharan desert, Atlantic Ocean, South America [*Torres et al.*, 1998; *Hsu et al*, 1999] and with aerosol mass concentrations, for example, those measured over the North Atlantic ocean [*Chiapello et al.*, 1999].

The long-term TOMS dataset from 1979 to present recorded from a succession of satellite platforms (Nimbus 7: 1979-1993; Meteor 3: 1991-1994; ADEOS: 1996-1997; Earth

Probe: 1996-present) provides a unique opportunity for an analysis of the long-term evolution of aerosol loading over the Indian subcontinent. Therefore, the objectives of this study include (a) a comparison of ground-based aerosol measurements and TOMS-Ai for individual stations, for evaluating quality of TOMS aerosol detection over India, (b) an analysis of the spatial and seasonal variability of absorbing aerosol load over India using TOMS Ai, and (c) a study of the interannual variability of absorbing aerosol loading during 1981-2000, over selected Indian regions characterized by different aerosol sources, and its relationship to regional meteorology and anthropogenic aerosol emissions.

2. Data base and methodology

2.1 TOMS aerosol product

TOMS has been designed for the estimation of the total-column ozone from the measured amount of backscattered UV radiance in six 1-nm wide wavelength bands (313, 318, 331, 340, 360 and 380nm) [*Herman et al.,* 1997]. At the three longest wavelength bands (340, 360 and 380 nm) gaseous absorption is weak, and the backscattered radiation is primarily governed by molecular scattering from aerosol and clouds [*Torres et al.,* 1998]. The algorithm for TOMS detection of aerosol and clouds from the backscattered UV radiance measurement is based on the residue theory described in *Herman et al.* [1997] and *Torres et al.* [1998]. The residue method is based on the principle that for a fixed 380 nm radiance the I_{340}/I_{380} spectral contrast is largest for non-absorbing aerosol and clouds and decreases with increasing absorption. UV absorbing aerosols (dust, smoke, soot) produce smaller contrast than predicted by pure Rayleigh scattering atmospheric model, consequently they yield positive residues. In contrast the non-absorbing aerosols (sulfate and sea-salt particles) produce greater contrast and negative residues. These positive or negative residues are termed as aerosol index (Ai).

Here, we consider only the positive values of TOMS Ai (hereafter TOMS Ai in this paper), corresponding to absorbing aerosol loading. The association of TOMS Ai with specific types of absorbing aerosols is largely based on the comparison of temporal and spatial variability of TOMS aerosol index (Ai) with known source of these aerosols [*Herman et al.*, 1997; *Seftor et al.*, 1997]. Four different TOMS instruments flew in space since November 1978 [*Herman et al.*, 1997]. Here we use TOMS data from Nimbus 7 for the years 1981-1992 and from Earth-Probe for the years 1997-2000. Since the latest instrument does not contain wavelengths at 340 and 380 nm, the aerosol index is calculated using the 330-360 nm range, the Ai being nearly a linear function of wavelength over the 330 and 360nm. It is recommended that TOMS Ai from Nimbus 7 (1981-1992) be scaled by a factor of 0.75 for comparison with those from Earth Probe (1997-2000) [*Hsu et al.*, 1999] and this is followed in the present work. However, as explained in a following section, our analysis shows that the data sets of TOMS Ai for the two periods, 1981-1992 and 1997-2000, were statistically from different populations, thus requiring separate analysis.

2.2 Ground-based measurement of aerosol optical depth

In order to compare TOMS Ai with ground-based AOD measurements over India, we compile measurements available from two networks in the Indian region, the Multi-Wavelength Solar Radiometer (MWR) network [*Moorthy et al.*, 1999] and the Aerosol Robotic Network (AERONET) [*Eck et al.*, 2001; *Holben et al.*, 2001].

For evaluating TOMS Ai against ground-based measurements on a monthly time-scale data were obtained from the MWR network, a network of sun photometers designed following the principle of filter wheel radiometers to make continuous spectral extinction measurements of ground-reaching, directly-transmitted solar flux at 10 narrow spectral bands. The extinction measurements are made in wavelength bands centered at 380, 400, 450, 500, 550, 600, 650, 700, 750, 800, 850, 935, and 1025 nm. Solar flux measurements are made using narrow interference filters with a maximum bandwidth of 6 to 10 nm [*Moorthy et al.*, 1999]. The raw data obtained using the MWR have been analyzed following the Langley plot technique and the columnar optical depth of the atmosphere is deduced at different wavelength bands [*Ramachandran et al.*, 1994; *Moorthy et al.*, 1999]. From the columnar optical depths, contributions of air molecule scattering and gaseous absorption relevant to the spectral bands have been subtracted using model values and columnar aerosol optical depth values have been reported. The reported AOD at 400 nm was chosen for this comparison to match closely with the wavelengths used to compute TOMS Ai.

The MWR instruments are operated only during clear days or on partly cloudy days when no visible clouds are present in the neighborhood of the solar disc. The data are scanty during the monsoon seasons when the sky is generally cloudy and overcast. In general the database is quite strong from November to March and poor for the period between June to September. The data have been averaged for each calendar month and provided by *Moorthy et al.* [1999]. The monthly-mean AOD data reported at four different locations (i.e. Thiruvananthapuram, Mysore, Vishakapatnam and Minicoy) are used in this study.

Uncertainties in the monthly-mean aerosol optical depths are from uncertainties in the model values used for air molecule scattering and molecular absorption, and from the averaging protocol for a given month and location. In general, data have been collected over a day for a minimum of 3-hour duration and used to obtain a single AOD value for the day. However, on some days and more frequently at some locations, the Langley plots revealed the existence of two slopes, one for the forenoon and one for the afternoon sessions [*Moorthy et al.*, 1999]. On these occasions the data were treated separately and AOD values for the forenoon and afternoon were calculated separately. Depending on sky conditions, therefore, the number of sessions per month in which data were collected varies between 5 and 15, but was occasionally as large as 30 or more at some locations. The standard error has been expressed as the standard deviation divided by square root of N (= number of days or day fragments in which AOD data were available and averaged). In general, the percent standard error in measured AOD at 400 nm was found to vary from 5-20% at Mysore and Vishakapatnam and from 5-40% at Thiruvananthapuram and Minicoy.

To evaluate the daily evolution of TOMS Ai, we compiled daily mean AOD measurements at 440nm, close to wavelengths used to compute TOMS Ai, from the Aerosol Robotic Network (AERONET) [*Eck et al.*, 2001], for a three month period from January-March 1999, corresponding to the intensive field phase of the INDOEX experiment. The two locations chosen were the Kaashidhoo Climate Observatory (KCO) at Maldives (4.9°N, 73.5°E), and the continental

station of Dharwar (15.4°N, 74.9°E) [*Leon et al*., 2001; *Reddy et al.*, 2004]. KCO is located about 700 km away from the Indian sub-continent without known proximate sources (Figure 1). Dharwar is a continental station close to the west coast of India, which receive air-mass from Northwest India Southern and Western parts of Asia (Figure 1). The TOMS pixel for the Dharwar station also covered Goa (15.5°N, 73.8°E), but the AERONET dataset was incomplete at Goa, thus leading to the choice of Dharwar for the inter comparison.

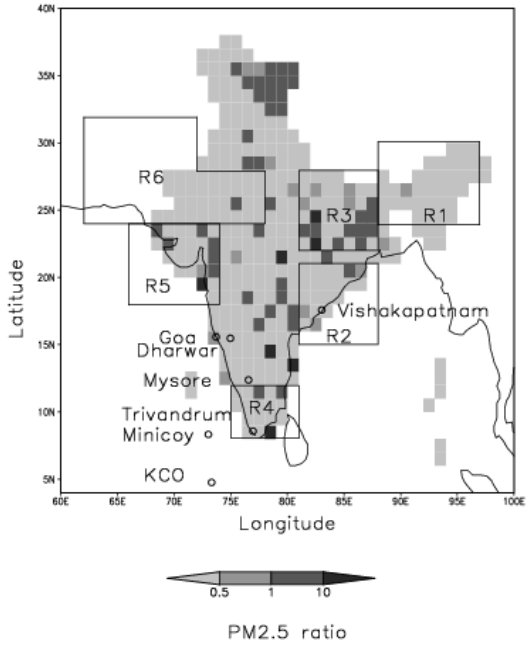

Figure 1.Ratio of $PM_{2.5}$ emission fluxes (kg $km^{-2}yr^{-1}$) from fossil fuel to biomass burning. Regions selected for analysis are R1 (24°-30° N; 88°-97° E), R2 (15°-21° N; 81°-88° E) dominated by biomass burning, R3 (22°-28° N; 81°-88° E), R4 (8°-12° N; 75°-81°E), and R5 (18°-24° N; 66°-74° E) dominated by fossil fuel and R6 (28°-32° N, 68°-72° E; 24°-28° N, 62°-78° E) desert dominated. The ground stations chosen for analysis of pollution events during INDOEX are Goa (15.5°N, 73.8°E), Dharwar (15.4°N, 74.9°E), Trivandrum (8.5°N, 76.9°E; coastal), Vishakapatnam (17.7°N, 83.2°E; industrialized) and Mysore (12.3° N, 76.5°E; continental), Minicoy (8.3°N, 73.1°E) and Kaashidhoo (4.9°N, 73.5°E).

2.3 Estimating absorbing aerosol emissions over India

To study the seasonal and interannual variability in absorbing aerosol load, in relation to emissions and regional meteorology, we chose six regions of India, dominated by emissions from different sources, i.e. biomass burning, fossil fuel combustion and desert dust.

2.3.1 Methodology for estimating aerosol emission trends and distributions

We classify anthropogenic absorbing aerosols to include black carbon (BC, predominantly from biomass burning in this region) and inorganic oxidized matter (IOM, mostly fly-ash from coal fired power plants, followed by mineral matter from open burning of crop waste and forests) [*Reddy and Venkataraman*, 2002a, b]. Soluble inorganic constituents like sulfate were not included in IOM. Detailed biofuel use for cooking [*Habib et al.*, 2004] are projected using national population for the period 1981-2000 from Government of India census data (http://www.censusindia.org.in). Crop waste generation trends are estimated from annual crop production for 1981-2000 [*Chanda et al.*, 2001] and related residue-to-product ratios [*Singh and Rangnekar,* 1986; *Bhatacharya et al.,* 1993; *Painuly et al.,* 1995; *Koopmans and Koppejan,* 1997]. Crop waste burnt in field is derived from the crop waste generated and the national average fraction burnt (i.e. crop waste burnt as a percentage of crop waste generated) 12% [*Reddy et al.*, 2002]. Literature-derived emission factors of BC and IOM for biofuel combustion [*Andreae and Merlet, 2001*; *Reddy and Venkataraman*, 2002b] crop waste open burning [*Reddy et al.*, 2002] and forest fires [*Reddy and Venkataraman*, 2002b] are used to estimate emission trends.

Fossil fuel use trends have been taken from CMIE [2001] for coal, low-speed and high-speed diesel, petrol (motor gasoline), fuel (furnace) oil, and kerosene [detailed in *Ramachandran and Jayaraman*, 2003]. Differences in emissions between this work and the detailed emission inventory for 1996 with emission factors based on technology and fuel consumption [*Reddy and Venkataraman*, 2002a], arose from the use of sector average emission factors by *Ramachandran and Jayaraman* [2003]. Scaling factors of 2.0 and 0.65 were applied respectively, to BC and IOM, to make the emissions trends of *Ramachandran and Jayaraman* [2003], for fossil fuels, consistent with the detailed inventory.

Climatological monthly mean BC emissions from forest fires have been derived by combining the source term with fire counts from ATSR (Along-Track Scanning Radiometer aboard satellite ERS-2) [*Reddy and Boucher*, 2004] averaged for the period 1996-2000, at a resolution of 1° x 1° over the Indian region. Forest burning is assumed to have negligible long-term variability and the climatological mean emissions of BC and IOM derived thus was added as a constant component to the national emissions during 1981-2000. However, for an analysis of interannual variability of TOMS Ai in northeast India (R1), variation in ATSR fire counts has been derived as monthly mean during 1997-2000 in this region. In spite of potential biases in the ATSR fire-counts, caused by pixel-size, nighttime and clear-sky sampling, this approach permits better representation of seasonal variations in forest burning on regional scales [*Duncan et al.*, 2003; *Generoso et al.*, 2003; *Reddy and Boucher*, 2004].

Spatial distributions of absorbing aerosol emissions are developed for the year 2000, using appropriate proxies to distribute state-level emissions to districts as done previously [*Reddy and Venkataraman*, 2002a, b] and gridded at a 1° x 1° resolution.

2.3.2 Sources and chemical composition of regional aerosol emission fluxes

We use the ratio of the gridded aerosol emissions for the year 2000, from fossil fuel to biomass burning, in order to identify the dominant sources of aerosols in each Indian region. Figure 1 shows low overall emission ratio from fossil fuels (light gray squares), suggesting that biomass burning sources (biofuel, crop waste open burning and forest fires) dominate most grids. However, sources like power plants, cement plants, refineries and iron and steel plants, dominate the emissions in several individual grids (dark gray and black squares in Figure 1). Northeast India (R1) and Bengal/Orissa (R2), chosen to represent biomass burning regions, are characterized by a large frequency of ATSR fire-count signals as shown in previous studies [*Duncan et al.*, 2003; *Reddy and*

Boucher, 2004]. Air-masses advected over the Indo-Gangetic plain (R3), south (R4) and west (R5), chosen as the fossil fuel dominated regions in this work, have been shown to contain high concentrations of anthropogenic aerosol constituents by recent field measurements [*Novakov et al.*, 2000; *Ramanathan et al.*, 2001; *Gabriel et al.*, 2002; *Mayol-Bracero et al.*, 2002]. A desert dust dominated region (R6) has been defined in the northwest of India, based on the dust emission inventory of *Tegen and Fung* [1995]. Figure 2 shows that the emission fluxes are the largest in the Indo-Gangetic plain (R3) followed by the other fossil fuel dominated regions (R4 and R5). The biomass burning regions (R1 and R2) exhibit lower emission fluxes, from their lower population density and industrialization, related to the predominantly forest land cover. The fossil fuel regions show significantly greater mixed sources (28-38% biomass contribution) than biomass burning regions (15-18% fossil fuel contribution). The desert dust dominated region, is characterized by a low anthropogenic emission flux, dominated by biomass burning. A large fraction of the anthropogenic $PM_{2.5}$ (or fine particle) emissions are contributed by absorbing anthropogenic aerosols (9-18% BC and 35-69% IOM) in the selected regions. Particulate matter emissions are dominated by carbonaceous aerosols in the biomass burning regions (R1 and R2) and by IOM in the fossil fuel regions (R3-R5). BC is emitted primarily from biomass burning in all regions. IOM matter is largely emitted from coal-fired utilities in the fossil fuel regions, while in the biomass dominated regions, it is emitted primarily from biofuel combustion in the northeast (R1), but from forest burning in the east (R2). Organic matter (OM) and BC emissions in India are strongly correlated, particularly from biomass burning and brick kiln dominated regions [*Reddy and Venkataraman*, 2002a, b] and may have an absorbing character [*Reddy and Boucher*, 2004; *Reddy et al.*, 2004]. This implies that the aerosols are likely to be chemically mixed.

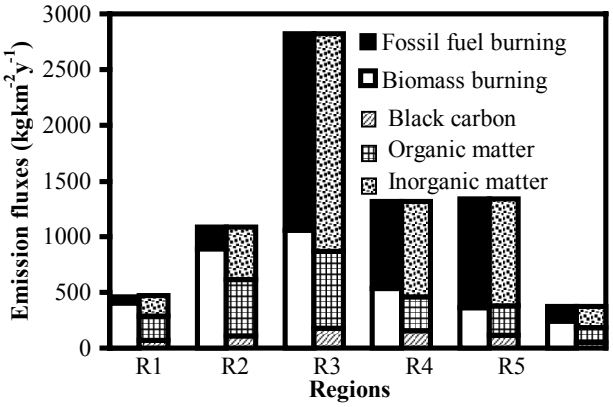

Figure 2. Emission fluxes (kg $km^{-2}yr^{-1}$) of (a) $PM_{2.5}$ and (b) aerosol chemical constituents in regions dominated by biomass burning (R1 and R2), fossil fuel combustion (R3, R4, and R5) and desert dust (R6).

2.4 Rainfall data

We analyze regional rainfall data, to examine the potential effect of rainfall on spatial and temporal variability of aerosol loading detected by TOMS. Rainfall in India is governed by the southwest monsoon (July-September), or Indian summer monsoon, which contributes to 77% of the annual national rainfall. *Gadgil et al.* [2002] have analyzed the SW monsoon using 130 years (1871-2001) of rainfall data and reported 70% of the years with normal rainfall, about 15% with drought and 15% with excess rainfall, and a strong natural variability. To analyze the effects of this variability on aerosol loading, rainfall data are obtained for 29 subdivisions of India (http://www.tropmet.res.in) for the 20-yr period (1981-2000). These data are compiled from a network of 306 rain gauge stations in the 29 meteorological subdivisions, which cover 90 percent of the total area of the country. In addition, the 100-yr average (1901-2000) of monthly mean rainfall is calculated in the selected regions. Monthly mean sub divisional rainfall is aggregated to derive the monthly mean rainfall and monsoon index (June-September rainfall, corresponding to the southwest monsoon) in selected regions.

2.5 NCEP data

To evaluate the potential effect of regional circulation changes on the aerosol load detected by TOMS, we analyze vertical velocity to identify regions with significant air-mass ascent, leading potentially to aerosol dispersion, or descent, leading to confinement of emissions, and possible higher aerosol loading. NCEP reanalysis data are downloaded from the web site of the NOAA-CIRES Climate Diagnostics Center, Boulder, Colorado, at http://www.cdc.noaa.gov. An examination of the monthly mean vertical velocity at 500 hPa and 850 hPa showed a significant seasonal and interannual shift in the regional circulation pattern. While the direction of vertical air-mass velocity at 850 and 500 hPa remained unchanged in most months, the spatial contrast was more clearly seen in the data at 500 hPa. Therefore, monthly mean vertical velocities at 500 hPa are used as an index of the dispersive potential of the atmosphere. The long-term average (1958-present) of monthly-mean vertical velocity over India typically ranged 0.02-0.06 Pa s^{-1}, with an interannual standard deviation between 0-0.02 Pa s^{-1}.

3. Results and Discussion

3.1 Comparison of TOMS aerosol index with ground-based AOD measurements

The stations from which long-term AOD measurements are used in this study include Thiruvananthapuram (8.5ºN, 76.9ºE), Mysore (12.3ºN, 76.5ºE), Vishakapatnam (17.7ºN, 83.2ºE), and Minicoy (8.3ºN, 73.1ºE), shown on Figure 1. It should be noted that the AOD data obtained during June 1991 to December 1993 were found to be influenced by Pinatubo volcanic aerosols [*Moorthy et al.*, 1996].

The correlation of monthly mean TOMS aerosol index with ground based monthly mean AOD at 400 nm is robust only at Vishakapatnam and Mysore (Figure 3). In terms of location, population, and industrial activity, Mysore can be characterized as a continental/rural site, while Vishakapatnam a coastal/industrialized site. Nevertheless, as shown in Figure 1, both Vishakapatnam and Mysore are located in regions dominated by biomass burning emissions, to which the positive TOMS spectral contrast is highly sensitive [*Hsu et al*, 1996; *Duncan et al.*, 2003]. The poorer correlation at Thiruvananthapuram and Minicoy (not shown) may result from several reasons. Thiruvananthapuram is located in a region dominated by fossil fuel emissions, and Minicoy, in an island of the Indian Ocean, dominated by sea-salt emissions (Figure 1), both with a significant scattering aerosol component. This overall mixed signal is likely to complicate the use of TOMS Ai at these sites [*Chiapello et al.*, 2000]. Also, the standard error in the ground-based AOD measurements is larger at these two sites potentially from

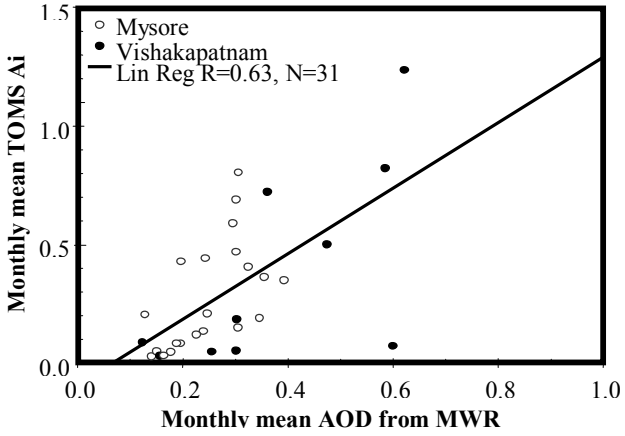

Figure 3. Scatter plot of monthly mean TOMS Ai with ground based monthly mean AOD at 400 nm at Mysore (open circles) and Vishakapatnam (filled circles).

variation in the sample size or number of sessions per month when AOD was recorded. This leads to differences in the time period of availability of AOD and TOMS Ai recorded per month and the averages thus obtained. Also, while data at the other sites were available for longer durations starting from 1987 or 1988 until May 1997, at Minicoy they were recorded only for a shorter duration, from January 1995 until May 1997. The factors complicate the comparison on ground-based and satellite-based measurements on a monthly mean time-scale.

We also examine the co-variability of AERONET derived AOD (440 nm) and TOMS Ai on a daily time-scale, during the January-March 1999 period of the Indian Ocean Experiment (INDOEX) at Dharwar and KCO (locations shown on Figure 1). TOMS Ai data are fewer in number than the AOD data since, as explained in Section 2.1, only positive Ai values were included, which correspond to absorbing aerosol loading. At Dharwar and KCO, the temporal evolution of daily TOMS Ai is relatively similar to AOD during Jan-Mar, 1999 (Figure 4a, b). Low daily TOMS Ai and AOD are observed at Dharwar between Jan 1st to Feb 15th (Figure 4a). The sharp and continuous increase during Feb 28th to Mar 30th, can be attributed to forest biomass burning based on analysis of ATSR fire counts during that period [*Léon et al.*, 2001]. The TOMS signal at KCO is generally low and noisy, probably due to the dominance of scattering sea-salt aerosols at this site (Figure 4b). However, a slight increase of TOMS Ai can be observed from Mar 14-30th, in consonance with the AOD increase during this period.

Therefore, reasonable agreement is seen between TOMS Ai and ground-based AOD measurements, on a monthly time-scale, at sites which lay in regions where biomass burning was predominant. The use of monthly-mean data presents difficulties related to correspondence in averaging time between TOMS Ai and ground based measurements, leading to discrepancies at several sites where the data were examined. At daily time scales, TOMS Ai is in good agreement with AOD measured at different AERONET sites during the three months of the INDOEX intensive field campaign. It is therefore recommended that daily mean data can be used to sufficiently capture the co-variation between satellite and ground based measurements.

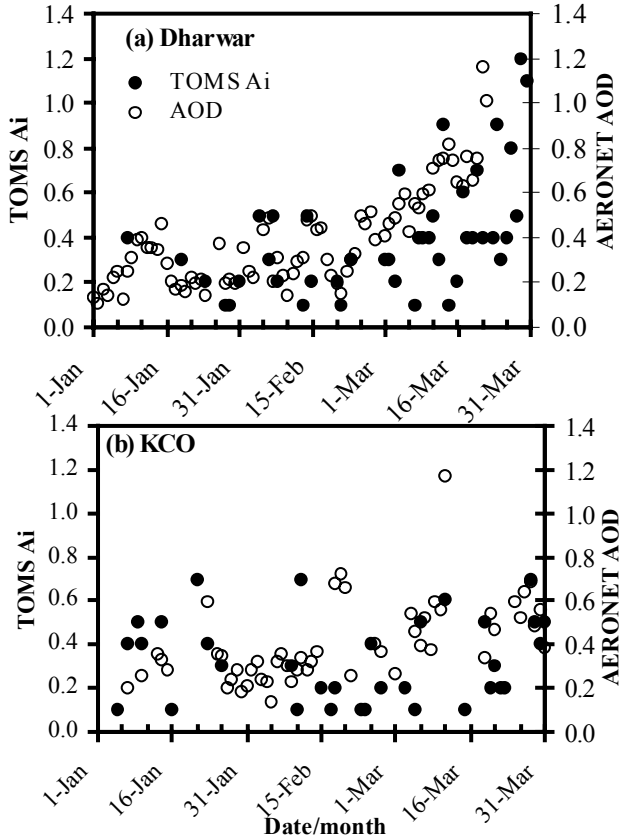

Figure 4 Daily mean TOMS Ai and AERONET AOD (440 nm) at ground stations (a) Dharwar (b) KCO during Jan-Mar 1999.

3.2 Seasonal and spatial variability in TOMS Ai

3.2.1 Spatial distributions in different seasons

Figure 5 shows the seasonal variability of TOMS Ai spatial distributions for the year 2000, for three periods of the year corresponding respectively to the NE-monsoon (Jan-Mar), the dry season (Apr-May) and the SW monsoon (Jun-Sept). In Oct-Dec (not shown), meteorological conditions are similar to Jan-Mar, however with some NE monsoon rainfall in south India. The spatial variability of TOMS Ai in each season is analyzed using absorbing aerosol emissions and potential aerosol sinks, like rainfall and atmospheric dispersion. Distributions of seasonal average rainfall over India are based on the data of year 2000. Monthly mean vertical air-mass velocities at 500 hPa from NCEP reanalysis data are used as an index of atmospheric dispersion, to identify regions with significant air-mass ascent, leading potentially to aerosol dispersion, or descent, leading to confinement of emissions, and possible higher aerosol loading.

During Jan-Mar, emissions distributions show large fluxes of anthropogenic absorbing aerosol emissions in Bengal (east), Indo-Gangetic plain, east coast plains and south India, with an additional peak in the west (Figure 5). However, the TOMS signal is low throughout and does not show a pattern similar to the emissions distributions. This difference cannot be explained by rainfall, which in this season is scanty over most of India. The circulation pattern, in terms of the estimated NCEP vertical velocity at 500 hPa, averaged for Jan-Mar 2000, shows significant air-mass ascent (purple and green) over the north Indo-Gangetic plain and descent (red) over central and eastern part of indo-Gangetic plain India.

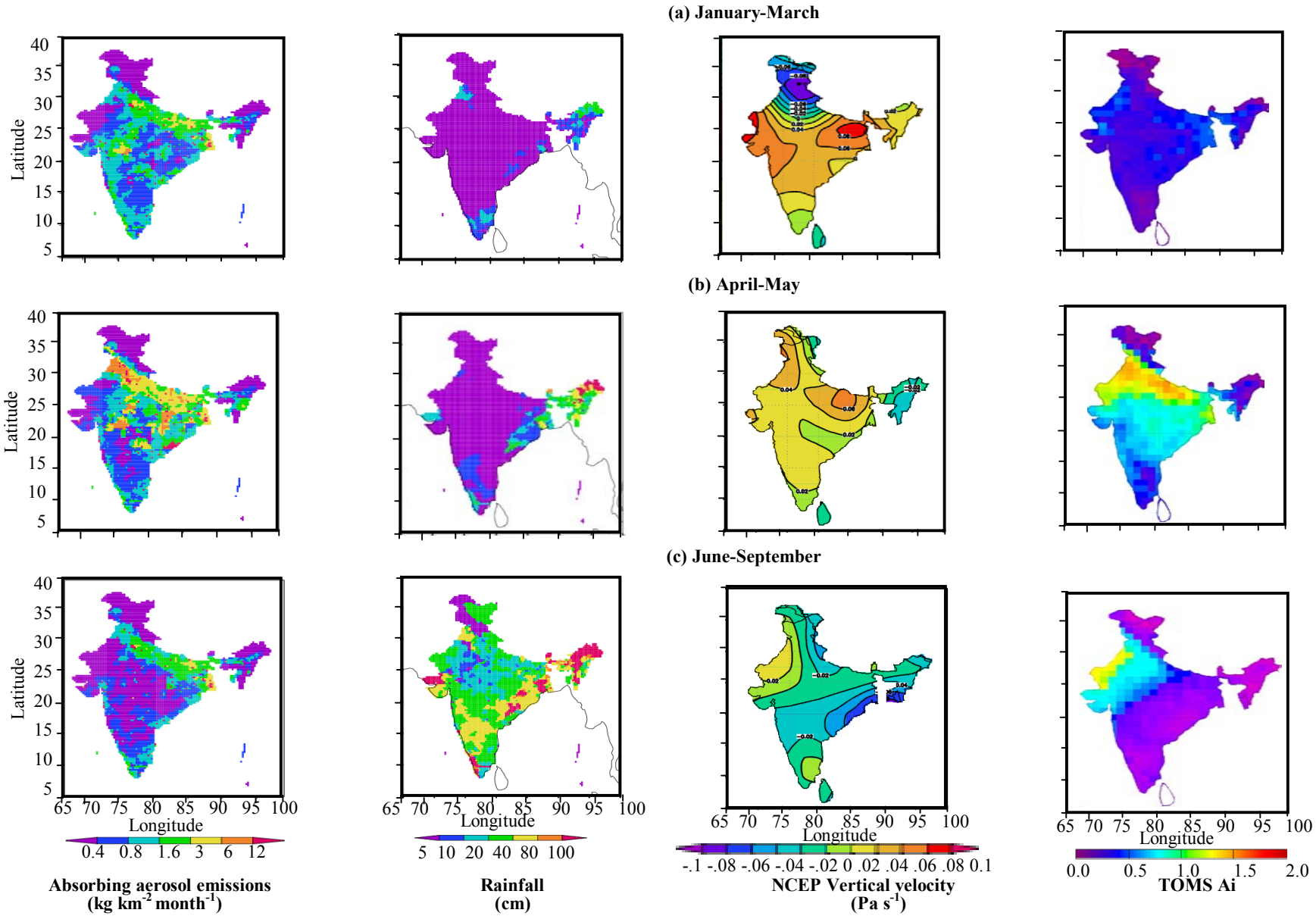

Figure 9. Seasonal variability in distributions of TOMS Ai, emissions of BC and IOM aerosols, rainfall and mean vertical velocity at 500 hPa over India, for the year 2000 during (a) NE-monsoon (Jan-Mar), (b) dry season (Apr-May), (c) SW-monsoon (Jun-Sep) and (d) winter (Oct-Dec) seasons.

The air-mass ascent over the Indo-Gangetic plain, could potentially result in significant dispersion of emissions from this region leading to the low absorbing aerosol loading detected by TOMS.

In the dry season (Apr-May), aerosol emissions from the Indo-Gangetic plain are accompanied by emissions from central India from forest fires and open burning of crop-waste. The TOMS signal shows corresponding high Ai over the Indo-Gangetic plain and northwest India. In this season once again there is insignificant rainfall over the subcontinent and insignificant aerosol removal through scavenging. The regional circulation pattern shows significant air-mass descent (red) over the Indo-Gangetic plain and northwest. This can potentially limit dispersion and lead to high loading of aerosols over the Indo-Gangetic plain, detected in the TOMS signal.

During the SW-monsoon (Jun-Sep), aerosol emissions continue to be high in the Indo-Gangetic plain and parts of south, and west India. However, TOMS Ai shows a low signal over the entire subcontinent, except for a high in the northwest. In this season, rainfall is generally high over most parts of India, especially west coast and the northeast and the circulation shows significant air-mass ascent over the Indian subcontinent, leading to high dispersion. The high TOMS Ai in the northwest is coincident with the desert region, where dust emission is active in March-June, in addition to the anthropogenic aerosol emissions shown in Figure 5. In addition, there is low-to medium rainfall in the northwest, and the circulation pattern also shows air-mass descent, with significant downward vertical velocities estimated in the NCEP data at 500 hPa. These factors combine to potentially lead to a high dust aerosol load, in northwest India during June-Sep, as measured by the high TOMS signal in this region. In Oct-Dec (not shown), the emissions and meteorological conditions are similar to Jan-Mar, and south India receives rainfall from the NE monsoon. TOMS Ai is low throughout the subcontinent during this season as in January-March.

Overall, the spatial distributions of absorbing aerosols detected by TOMS, exhibit a relation to emissions distributions on a sub-continental scale, when rainfall and dispersion are insignificant, for example, Apr-May. However, atmospheric dispersion on a regional scale (as in Jan-Mar over north India) and rainfall (as in June-Sep) reduce aerosol loads and modify their spatial distributions in relation to their emissions.

3.2.2 Monthly variability in selected regions

Monthly mean TOMS Ai are extracted and spatially averaged over the six selected regions shown in Figure 1, dominated by different aerosol sources, and described in Section 2.3. As explained earlier, TOMS Ai from Nimbus 7 (1981-1992) were scaled by the recommended factor of 0.75 for direct comparison with those derived from TOMS/Earth Probe (1997-2000) [*Hsu et al*, 1999]. In spite of this, in all selected regions, the datasets from Nimbus 7 and Earth Probe, when tested using a t-test, at 95% statistical significance, were seen to come from different populations, not making it possible to pool the datasets in our analysis. Therefore, in all the following sections, the data sets from 1981-1992 and 1997-2000 are treated separately.

Figure 6 shows the monthly mean TOMS Ai spatially averaged over each region for the period 1981-1992, with one standard deviation shown by error bars. Also shown in each region, is the monthly mean rainfall, averaged over the same period, using the rainfall data described in Section 2.4, from the meteorological subdivisions corresponding to each region. The northeast and east (R1 and R2) are dominated by biomass burning emissions (Figure 2), of which biofuel combustion emissions are invariant with season, and open burning emissions are predominant in March-May. The peak TOMS Ai in the northeast is in April, when onset of rainfall reduces the aerosol load. In the east (R2), the peak TOMS Ai is in May, from the later onset of rainfall in June, after which once again, the increasing rainfall decreases aerosol load. The Indo-Gangetic plain (R3) has the largest absorbing aerosol fluxes among the six regions, with about 60% from fossil fuel combustion, typically invariant with season, and 40% from biomass burning (Figure 2), thus with an expected lower seasonal variation in emissions than east or northeast. However, the similar monthly rainfall distribution in the Indo-Gangetic plain, to that in the east, results in a seasonal cycle in TOMS Ai very similar to that in the east. The south (R4) is has mixed emissions with almost equal fluxes from biomass and fossil fuel burning (Figure 2). The distinct features of this region include a harvest season in Jan-Feb, leading to potential open burning emissions in these months, and the influence of both southwest and northeast monsoon rainfall. The peak rainfall in this region is 100-200 cm month^{-1}, lower than in R1-R3, but persisting from June-November. The peak TOMS Ai has a lower value than in R2 and R3, from the lower emissions flux in this region. It occurs in May, but does not fall off sharply as the rainfall amounts are lower than in the other regions. The west and northwest have lower anthropogenic aerosol fluxes (Figure 2), but experience high dust load from the Thar desert, along with more scanty rainfall than the other regions. High dust activity typically occurs in May-June. The seasonal cycle in TOMS Ai thus shows enhanced peak values in June, especially in the northwest, which is affected more by desert dust. The onset of rainfall in both regions is from July leading to a steady reduction in TOMS Ai. The combination of high dust load and low rainfall induces the largest values of TOMS Ai in these two regions. Therefore, the magnitude of TOMS Ai bore a relation to anthropogenic aerosol emission strength in all regions except those with a strong desert dust loading. The seasonal cycle in TOMS Ai was related primarily to the seasonal variability in dust or open burning emissions and a large influence of rainfall in reducing the aerosol load.

3.3 Interannual variability in TOMS Ai

In the following discussion we analyze the year-to-year variability of the Apr-May mean TOMS Ai, which is always higher than the annual mean (Figure 7) TOMS Ai and governs the annual mean in each region. Using the 1981-1992 data, the largest TOMS Ai is observed in the desert dust dominated region (R6, 1.00±0.16), which result both from local dust emissions and potentially from long-range transport from the Arabian and Saharan desert regions, known to be active during Apr-May [*Satheesh and Srinivasan*, 2002]. Moreover, TOMS Ai is more sensitive to dust aerosols and to aerosols at higher altitudes [*Herman et al.*, 1997; *Torres et al.*, 1998] potentially contributing to the high TOMS Ai recorded in this region. Among regions dominated by anthropogenic emissions, TOMS Ai follows trends in the magnitude of absorbing aerosol emission flux (Figure 2), with highest TOMS Ai in the Indo-Gangetic plain (R3, 0.92±0.19) followed by east and west (R2, 0.72±0.17; R5, 0.66±0.20),

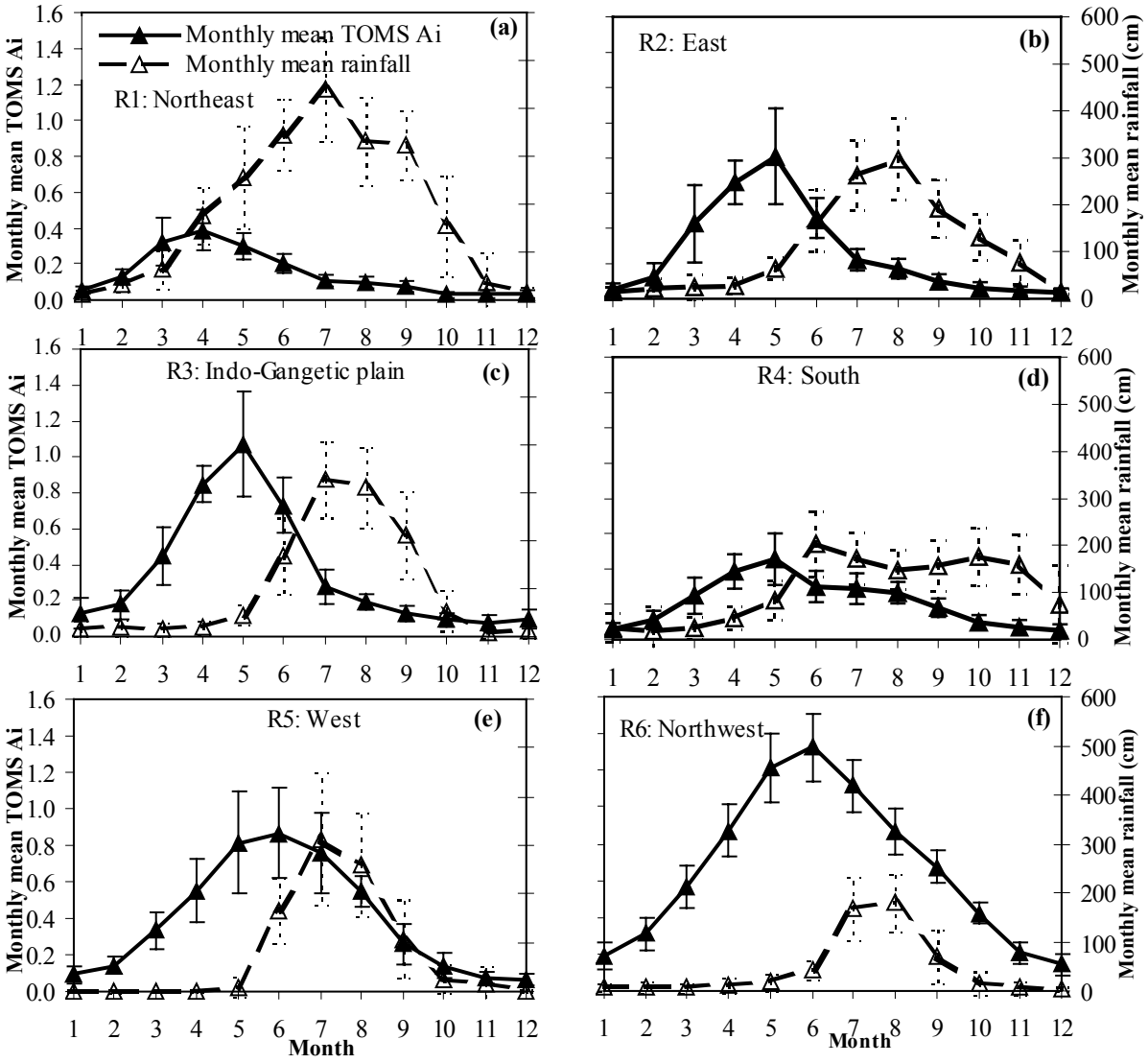

Figure 6. Seasonal cycle in the TOMS Ai (solid lines with filled triangles) and in rainfall (dotted lines with open triangles) in regions dominated by biomass burning (R1 and R2), fossil fuel combustion (R3, R4, R5) and desert dust (R6).

and significantly lower in the south and northeast (R4, 0.40±0.10; R1, 0.32±0.09).

3.3.1. Influence of meteorology

Figure 7 shows similarities in the interannual trends of TOMS Ai in the different regions, thus suggesting the influence of common meteorological phenomena on a sub-continental scale. High April-May mean TOMS Ai (Figure 7) is observed in 1984, 1985, 1988, 1991 and 1999, in most regions. In contrast, low TOMS Ai is seen in 1981, 1982, 1987, 1990 and 1997 in several regions. These highs and lows are more marked in the east, Indo-Gangetic plain, west and northwest.

The effects of regional circulation changes and variability in rainfall are examined as potential contributors to the interannual variability in TOMS Ai. As in Section 3.2.1, the vertical velocity at 500 hPa was used as an index of atmospheric dispersion, with upward or downward vertical velocity, respectively, potentially reducing or increasing the aerosol load at that location. The composite mean vertical velocity at 500 hPa was calculated for five year sets of high (1984+1985+1988+1991+1999) and low (1981+1982+1987+1990+1997) TOMS Ai, and their difference is shown in Figure 8. Significant downward air-mass velocities were seen in the years of high TOMS Ai compared to those of low TOMS Ai, extending over the entire northern part of the sub-continent covering the east, Indo-Gangetic plain, west and northwest regions, in which the corresponding differences in TOMS Ai were observed. The difference, shown in Figure 8, ranges 0.02-0.08 Pas^{-1} over north India while the standard deviation in the long-term mean vertical velocity ranged 0-0.02 Pas^{-1} in this region. This suggests statistical significance in the difference in composite mean vertical velocities between the years of high and low aerosol loading as detected by TOMS. This analysis suggests a link between regional circulation anomalies and those in the aerosol load detected by TOMS.

The role of increases in rainfall-related soil moisture and ground cover, on potentially reducing aerosol loads, is examined for all the regions using a correlation between annual rainfall in a given year (year n) with TOMS-Ai in the

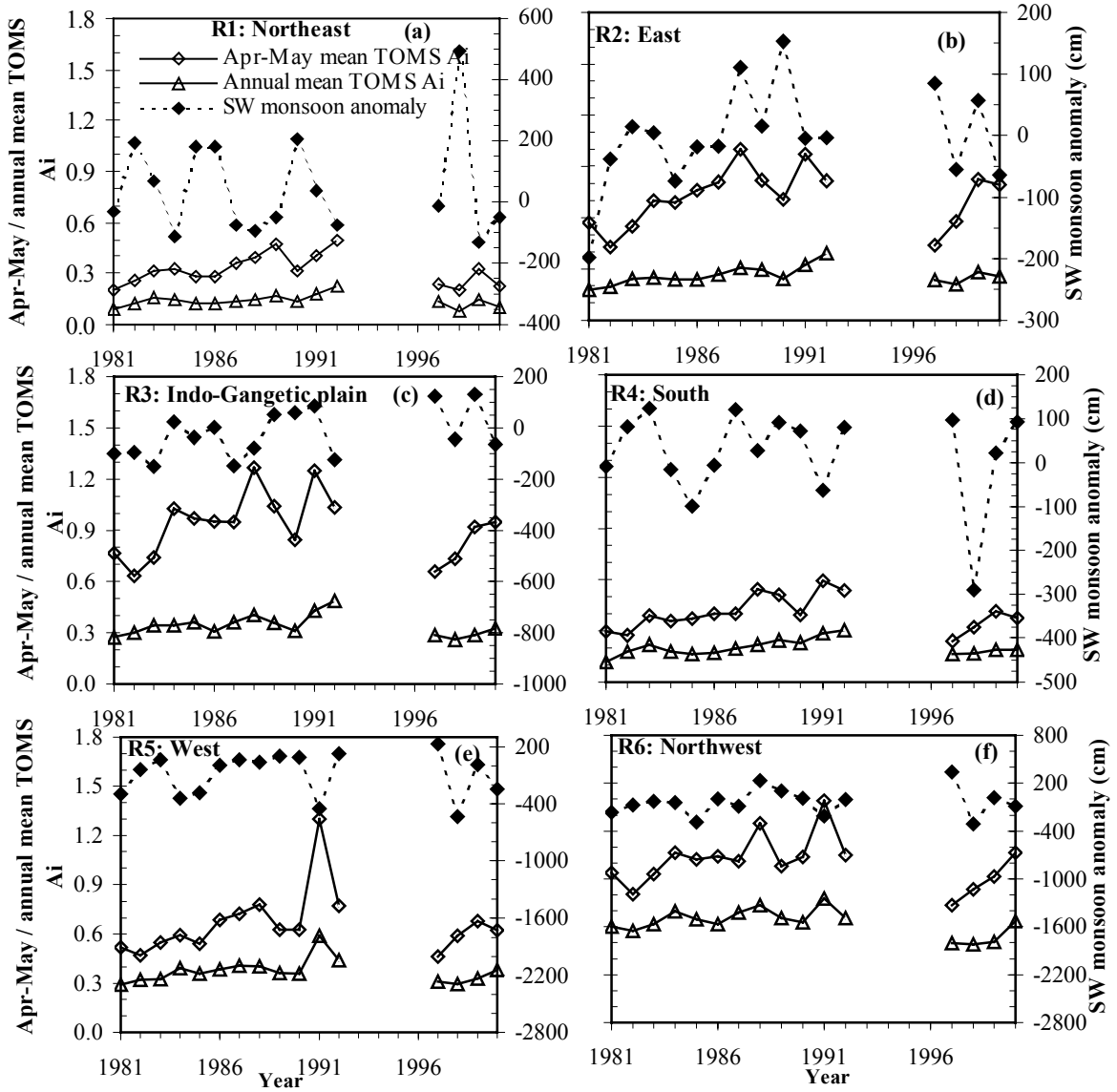

Figure 7. Regional analysis of variation in TOMS Ai, as a percentage from the trend mean, and that SW monsoon rainfall, from the 100-yr mean of 1900-2000 (SW monsoon rainfall anomaly).

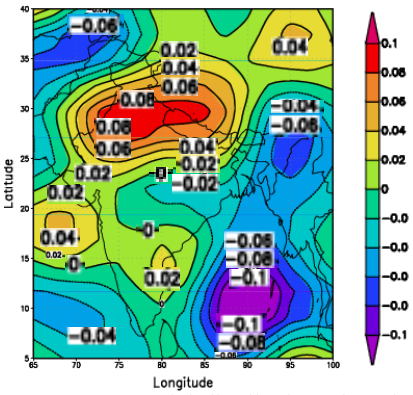

Figure 8. Spatial distribution of vertical velocity (Pa s^{-1}) at 500hPa for years when TOMS Ai exhibited a sub-continental highs and lows (a) difference in vertical velocities between high in 1984, 85, 88, 91, 99 and lows in 1981, 82, 87, 90, 97.

following year (year n+1). The expected negative correlation was not statistically significant in any region, possibly because anthropogenic rather than dust aerosols are expected to dominate the atmospheric aerosol load in all regions but for the northwest (R6).

We examine the potential effect of variability in aerosol load in the pre-monsoon months of April-May, as represented by TOMS Ai, on the variability in SW monsoon rainfall. In the six selected regions, TOMS Ai is plotted along with the difference in SW monsoon rainfall from its 100-yr mean (1900-2000) in the region, termed monsoon anomaly (Figure 7). In several years of high TOMS Ai, for example 1984-85 and 1991, a decrease is seen in SW monsoon rainfall in regions of India including the south, west and northwest. In contrast, in 1982 and 1990, the low TOMS Ai is accompanied by increased SW monsoon rainfall in the northeast, east and south. We suggest that this co-variation is consistent with monsoon thermodynamics [e.g. *Srinivasan*, 2001], which relates precipitation to evaporation, the integrated column water vapor content and net change in the top-of-atmosphere

radiation flux. The shift in regional circulation from greater air-mass descent in the years of high TOMS Ai, would lead to drier conditions and lower surface convection. In addition, the high absorbing aerosol load in these years, would reduce net downward radiative flux at the surface, and could reduce evaporation and the column water vapor content, thus reducing precipitation. Further, atmospheric heating by absorbing aerosols could reduce the atmospheric temperature lapse rate leading to greater atmospheric stability and weaker monsoon activity. As we have qualitatively analyzed a limited dataset here, the correlation seen of aerosol loading with regional circulation and the monsoon is illustrative, and should not be used to conclude a causative effect of aerosols on monsoon variability.

3.3.2. Influence of emissions

Figure 7 shows that during the period 1997-2000 the interannual variability of TOMS Ai in the northeast region R1, is characterized by exceptionally high TOMS Ai during 1999, about 3 times larger than in the other adjacent years This region is known to be affected by forest biomass burning, with ATSR fires in 1999 seen to feature an intense area of burning along the foothills of the Himalaya in the Indo-Gangetic plain [*Duncan et al.*, 2003, *Reddy and Boucher*, 2004]. Variability in forest burning emissions is thus examined as a potentially dominant contributor to TOMS Ai in the northeast region. Monthly mean ATSR fire counts are derived for 1997-2000 in this region (Figure 9) and ranged from 5 to 30 during March-May in 1997, 1998, and 2000 but recorded an exceptional peak of 329 during March 1999 (24 in April and 3 in May 1999). It should be noted that from July to December, ATSR detected no fires in this region, in contrast to the low, but still positive values of TOMS Ai during these months. While ATSR fire-counts may be biased from pixel size, clear-sky and night-time sampling [*Arino et al.*, 2001], the co-variation with TOMS Ai observed here, points to the role of BC emissions from forest fires in enhancing TOMS Ai in northeast India in 1999.

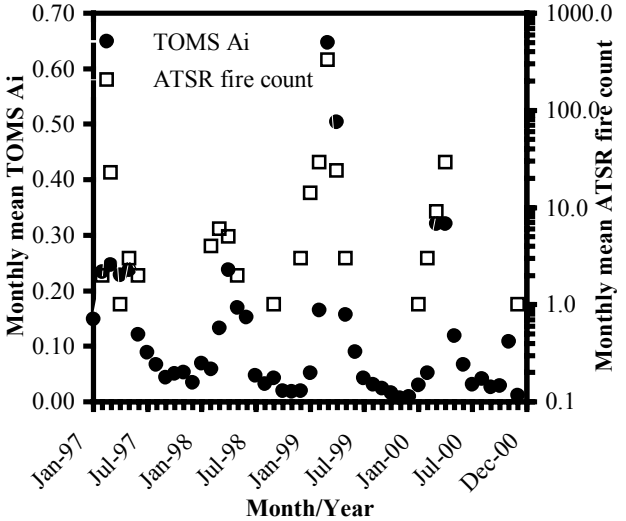

Figure 9. Monthly mean of TOMS Ai and ATSR fire counts (excluding zero values) in the Northeast region R1 dominated by open biomass burning from 1997 to 2000.

As meteorological parameters allow only to partially explain the interannual variability of TOMS-Ai, we examine the influence of the variability of absorbing aerosol emissions, projected during 1981-2000, as described in Section 2.3. These projections (Figure 10) show an increase in average emissions of BC from 270 in 1981 to 450 Gg in 2000 (i.e. a factor 1.6) and of IOM from 1100 in 1981 to 2500 Gg in 2000 (i.e. a factor 2.3). The increase in emissions from biomass burning of about 2% yr^{-1} is reflected by the growth rate in user population of biofuels (i.e. the rural population) and the increase in crop waste burnt as a function of growth in crop production during this period. Forest emissions were assumed invariant at the mean value estimated for 1996-2000. The increase in emissions from fossil fuel burning of about 9% yr^{-1} reflects an increase in industrial fossil fuel use, with BC being governed by diesel transport and IOM by coal use in electric power generation. These national average emissions are distributed to the six regions, based on the regional distribution of emissions for the year 2000. While this approach assumes an invariant spatial distribution of emissions during the 20 year period, we believe it offers a reasonable first approximation of the decadal growth in regional emissions.

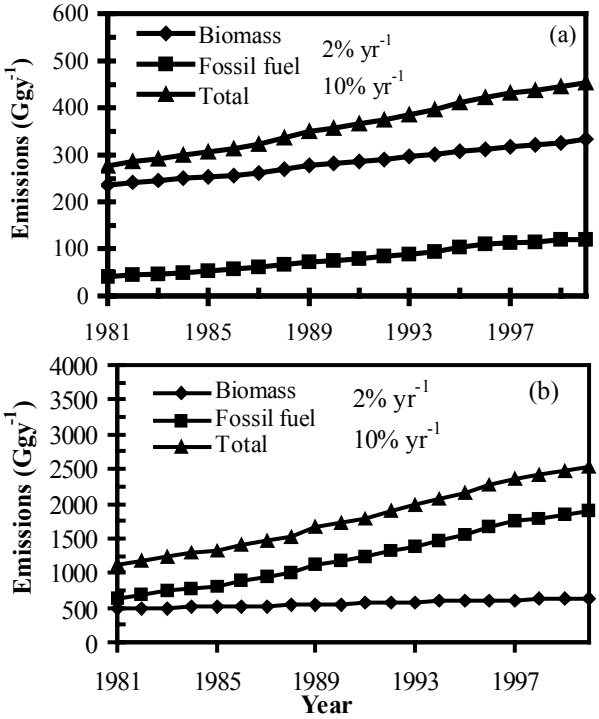

Figure 10. Long-term trends in emissions of (a) BC and (b) IOM from fossil fuel and biomass combustion for India during 1981-2000.

To arrive at the dependence of the year-to-year TOMS Ai on annual mean emissions, circulation effects and rainfall, a dataset is developed for each region of annual emissions, as described above, of NCEP vertical velocity at 500 hPa for Apr-May and of annual rainfall of the previous year, for the years 1981-1992. Interannual variability in TOMS Ai is examined simultaneously in relation to that in anthropogenic aerosol emissions, vertical velocity and rainfall from the year (n-1), using a multiple regression (Table 1). The interannual variability in TOMS Ai in all regions is explained to the largest extent (37-70%) by trends in anthropogenic aerosol emissions. Atmospheric circulation, in terms of vertical velocity, is not useful in explaining year-to-year variability in

Table 1 Dependence of TOMS Ai on absorbing aerosol emissions, vertical velocity and annual rainfall (year n-1)

Regions	% Contribution to variability in TOMS Ai				R^2	F[a]	Significance-F[b]
	Emissions	Vertical velocity	Rainfall	Unexplained			
R1	70	5	8	18	0.82	12	0.002
R2	56	0	5	38	0.62	4	0.044
R3	42	0	11	47	0.53	3	0.092
R4	73	1	4	21	0.79	10	0.005
R5	46	2	0	51	0.49	3	0.131
R6	37	1	7	55	0.45	2	0.163

[a]F is the ratio of the regression mean square to the residual mean square. [b]F-significance is less than 0.05 then the hypothesis that there is no (linear) relationship can be rejected, and the multiple correlation coefficient can be called statistically significant.

TOMS Ai. Rainfall from the (n-1) year could reduce dust emissions and forest fires in the following year (n) from enhanced soil and vegetation moisture. This could be a potential mechanism for the variability in rainfall having a significant effect on TOMS Ai in the northeast (R1, a biomass burning region) and northwest (R6, desert region). However, a mechanism is not apparent for the effect of rainfall on TOMS Ai in the Indo-Gangetic plain (R3). We conclude that increasing anthropogenic aerosol emissions, especially those from fossil fuel combustion at a high rate of 9-10% y^{-1} over the 1981 values, significantly affect the absorbing aerosol load detected by TOMS, in all selected regions of study.

4.0 Conclusions

This study presents an analysis of seasonal, spatial and interannual variability in absorbing aerosol loading over India, detected by TOMS during 1981-2000, in relation to estimated anthropogenic aerosol emission trends and regional meteorology, including rainfall and circulation patterns. The agreement between TOMS Ai and ground-based AOD data, was reasonable on a monthly time-scale, and good on a daily time-scale, leading to the recommendation of daily-mean data to sufficiently capture the co-variability in ground-based and satellite-based measurements. Seasonal and spatial distributions in TOMS Ai were related to the emission patterns in Apr-May, but modified by regional atmospheric dispersion in Jan-Mar and rainfall in Jun-Sep. The magnitude of TOMS Ai bore a relation to anthropogenic aerosol emission strength in all regions except those with a strong desert dust loading. The seasonal cycle in TOMS Ai corresponded to the seasonal variability in dust or open burning emissions and to rainfall. A link between regional circulation anomalies and those in the aerosol load detected by TOMS, was suggested by significant downward air-mass velocities, estimated in the NCEP reanalysis data, in years of high TOMS Ai compared to those of low TOMS Ai, extending over the entire northern part of the sub-continent covering the east, Indo-Gangetic plain, west and northwest, potentially resulting in low atmospheric dispersion and higher aerosol load detected by TOMS. In several years, high TOMS Ai correlated with a decrease in SW monsoon rainfall in the south, west and northwest, while low TOMS Ai correlated with an increase in SW monsoon rainfall in the northeast, east and south, consistent with monsoon thermodynamics. This relation is however only illustrative, because of the small data set analyzed here. Enhanced TOMS Ai in 1999 in northeast India, was potentially from forest burning emissions, deduced from its strong correlation with ATSR fire counts in this region. Large increases in anthropogenic aerosol emissions from India during 1981-2000, especially from fossil fuel use, significantly explain the interannual variability in aerosol loading detected by TOMS over most regions of India.

Acknowledgments

This work was supported by the Indo-French Centre for the Promotion of Advanced Research (IFCPAR). Additional investigator support (GH and CV) was provided by the Geosphere-Biosphere program of Indian Space Research Organization (ISRO-GBP). Chandra Venkataraman's visit to LOA in May, 2004, was supported through the Indo-French Collaboration Program of the Embassy of France in India.

References

Anderson, T. L., et al., Climate forcing by aerosol-a hazy picture, *Science*, *300*, 1103-1104, 2003.

Arino, O., M. Simon, I. Piccolini, and J. M. Rosaz, The ERS-2 ATSR-2 world fire atlas and the ERS-2 ATSR-2 world burnt surface atlas projects, *Proceedings of the 8th ISPRS conference on physical measurement and signatures in remote sensing*, Aussois, 8-12 Jan., 2001.

Bhattacharya, S. C., H. L. Pham, R. M. Shrestha, and Q. V. Vu, CO_2 emissions due to fossil and traditional fuels, residues and wastes in Asia, paper presented in AIT Workshop on Global Warming Issues in Asia, 8-10 September 1992, AIT, Bangkok, Thailand, 1993.

Boucher, O., and J. Haywood, On summing the components of radiative forcing of climate change, *Climate Dyn.*, *18*, 297-302, 2001.

Chanda, T. K., A. C. Dubey, K. Sati, and C. Robertson, Fertilizer Statistics 2000-2001, *rep.*, 434 pp., Fertilizer Association of India, New Delhi, 2001.

Chowdhury, Z., L. S. Hughes, L. G. Salmon, and G. R. Cass, Atmospheric particle size and composition measurements to support light extinction calculations over the Indian Ocean, *J. Geophys. Res., 106*, 28,597-28,605, 2001.

Chiapello, I., J. M. Prospero, R. Herman, and N. C. Hsu, Detection of mineral dust over the North Atlantic Ocean and Africa with the Nimbus 7 TOMS, *J. Geophys. Res.*, *104*, 9277-9291, 1999.

Chiapello, I., P. Goloub, D. Tanré, and A. Marchand, Aerosol detection by TOMS and POLDER over oceanic regions, *J. Geophys. Res.*, *105*, 7133-7142, 2000.

CMIE, Economic intelligence service: Energy center for monitoring Indian economy Pvt. Ltd. India, 2001.

Duncan, B. N., R. V. Martin, A. C. Staudt, R. Yevich, and J. A. Logan, Interannual and seasonal variability of biomass burning emissions constrained by satellite observations, *J. Geophys. Res.*, *108*(D2), 4100, doi:10.1029/2002JD002378, 2003.

Eck, T. F., et al., Column-integrated aerosol optical properties over the Maldives during the northeast monsoon for 1998-2000, *J. Geophys. Res., 106*, 28,555-28,566, 2001.

Gabriel, R., O. L. Mayol-Bracero, and M. O. Andreae, Chemical characterization of submicron aerosol particles

collected over the Indian Ocean, *J. Geophys. Res.*, 107(D19), 8005, doi:10.1029/2000JD000034, 2002.

Gadgil, S., J. Srinivasan, R. S. Nanjundiah, K. K. Kumar, A. A. Munot, and K. R. Kumar, On forecasting the Indian summer monsoon: the intriguing season of 2002, *Curr. Sci., 83*, 394-403, 2002.

Generoso, S., F.-M. Bréon, Y. Balkanski, O. Boucher, and M. Schulz, Improving the seasonal cycle and interannual variations of biomass burning aerosol sources, *Atmos. Chem. Phys., 3,* 1211-1222, 2003.

Habib, G., C. Venkataraman, M. Shrivastava, R. Banerjee, J. Stehr and R. Dickerson, New methodology for estimating biofuel consumption in India: Atmospheric emissions of black carbon and sulfur dioxide, *Manuscript submitted to Global Biogeochem. Cyc.*, 2004.

Herman, J. R., P. K. Bhartia, O. Torres, C. Hsu, C. Seftor, and E. Celarier, Global distribution of UV-absorbing aerosols from Nimbus 7/TOMS data, *J. Geophys. Res.*, *102*, 16911-16922, 1997.

Holben et al., AERONET-A federated instrument network and data archive for aerosol characterization, *Remote Sens. Environ., 66,* 1-16, 1998.

Hsu, N. C., J. R. Herman, P. K. Bhartia, C. J. Seftor, O. Torres, A. M. Thompson, I. F. Gleason, T. F. Eck, and B. N. Holben, Detection of biomass burning smoke from TOMS measurements, *Geophys. Res. Lett.*, *23*, 745-748, 1996.

Hsu, N. C., et al., Comparison of the TOMS aerosol index with sun photometer aerosol optical thickness: Results and applications, *J. Geophys. Res.*, *104*, 6269-6279, 1999.

Husar, R. B., J. M. Prospero, and L. L. Stowe, Characterization of tropospheric aerosols over the oceans with the NOAA advanced very high resolution radiometer optical thickness operational product, *J. Geophys. Res.*, *102*, 16,889-16,910, 1997.

Koopmans, A. and J. Koppejan, Agricultural and forest residues-generation, utilisation and availability, paper presented at the regional consultation on modern applications of biomass energy, Kuala Lumpur, Malaysia, 6-10 January 1997.

Leon, J.-F., et al., Large-scale advection of continental aerosols during INDOEX, *J. Geophys. Res., 106*, 28,427-28,439, 2001.

Li, F., and V. Ramanathan, Winter to summer monsoon variation of aerosol optical depth over the tropical Indian Ocean, *J. Geophys. Res.*, *107*(D16), 4284, doi:10.1029/2001JD000949, 2002.

Mayol-Bracero, O. L., et al., Carbonaceous aerosols over the Indian Ocean during the Indian Ocean Experiment (INDOEX): Chemical characterization, optical properties, and probable sources, *J. Geophys. Res., 107*(D19), 8030, doi:10.1029/2000JD000039, 2002.

McPeters, R. D. et al., Nimbus-7 Total ozone mapping spectrometer (TOMS) data products user guide, *NASA Ref. Publ.*, 1384, 1996.

Moorthy, K. K., P. R. Nair, B. V. Krishna Murthy, and S. K. Satheesh, Time evolution of the optical effects and aerosol characteristics of Mt. Pinatubo origin from ground based observation, *J. Atmos. Terr. Phys.*, *58*, 1101-1116, 1996.

Moorthy, K. K., K. Niranjan, B. Narasimha Murthy, V. V. Agashe, and B. V. Krishna Murthy, Aerosol Climatology over India, *Rep. ISRO GBP SR 0399*, pp. 70, Indian Space Research Organization, India, 1999.

Moorthy, K. K., Aerosol climatology and effects: Network activity, climatology and trends, *Proceedings of the working group on atmospheric chemistry aerosols and global change,* Space physics laboratory India, pp. 56, 2001.

Moorthy, K. K., A. Saha, B. S. N. Prasad, K. Niranjan, D. Jhurry, and P. S. Pillai, Aerosol optical depths over India and adjoining ocean during the INDOEX campaigns: Spatial, temporal, and spectral characteristics, *J. Geophys. Res.*, *106*, 28,539-28,554, 2001.

Novakov, T., M. O. Andreae, R. Gabriel, T. W. Kirschstetter, O. L. Mayol-Bracero, and V. Ramanathan, Origin of carbonaceous aerosols over the tropical Indian Ocean: Biomass burning or fossil fuels? *Geophys. Res. Lett., 27*, 4061-4064, 2000.

Painuly, J. P., H. Rao and J. Parikh, A rural energy-agriculture interaction model applied to Karnataka state, *Energy*, 20(3), 219-233, 1995.

Ramachandran, S., A. Jayaraman, Y. B. Acharya, and B. H. Subbaraya, Features of aerosol optical depths over Ahmedabad as observed with a Sun-tracking photometer, *Contr. Atmos. Phys.*, *67*, 57-70, 1994.

Ramachandran, S., and A. Jayaraman, Premonsoon aerosol mass loadings and size distribution over Arabian Sea and tropical Indian Ocean, *J. Geophys. Res.*, *107*(D24), 4738, doi:10.1029/2002JD002386, 2002.

Ramachandran, S., and A. Jayaraman, Ballon-borne study of the upper tropospheric and stratospheric aerosols over a tropical station in India, *Tellus*, *55B*, 820-836, 2003.

Ramanathan, V., et al, Indian Ocean Experiment: An integrated analysis of the climate forcing and effects of the great Indo-Asian haze, *J. Geophys. Res.*, *106*, 28,371-28,398, 2001.

Rasch, P., W. Collins, and B. Eaton, Understanding the Indian Ocean Experiment (INDOEX) aerosol distributions with an aerosol assimilation, *J. Geophys. Res.*, *106*, 7337–7356, 2001.

Reddy, M. S., and C. Venkataraman, A 0.25^o x 0.25^o inventory of aerosol and sulfur dioxide emissions from India: I-Fossil fuel combustion, *Atmos. Environ.*, *36*, 677-697, 2002a.

Reddy, M. S., and C. Venkataraman, A 0.25^o x 0.25^o inventory of aerosol and sulfur dioxide emissions from India: II – Biomass combustion, *Atmos. Environ.*, *36*, 699-712, 2002b.

Reddy, M. S., O. Boucher, and C. Venkataraman, Seasonal carbonaceous aerosol emissions from open biomass burning in India, *Bull. IASTA*, *14*(1), 239-243, 2002.

Reddy, M. S., and O. Boucher, A study of global cycle of carbonaceous aerosols in the LMDZT general circulation model, submitted to *J. Geophys. Res.*, 2004.

Reddy, M. S., O. Boucher, C. Venkataraman, S. Verma, J.-F. Leon, and M. Pham, GCM estimates of aerosol transport and radiative forcing during INDOEX, submitted to *J. Geophys. Res.*, 2004.

Satheesh, S. K., and J. Srinivasan, Enhanced aerosol loading over Arabian Sea during the pre-monsoon season: natural or anthropogenic?, *Geophys. Res. Lett.*, *29(18)*, 1874, 10.1029/2002GL015687, 2002.

Seftor, C. J., N. C. Hsu, J. R. Herman, P. K. Bhartia, O. Torres, W. I. Rose, D. J. Schneider, and K. Krotkov, Detection of volcanic ash clouds from Nimbus-7/total ozone mapping spectrometer, *J. Geophys. Res.*, *102*, 16,749-16,759, 1997.

Singh, K. and D. V. Rangnekar, Fibrous crop wastes as Animal feeds in 1986 India. In Rice straw and related feeds

in Ruminants ration. *Proc. International Workshop held in Kandy, Sri Lanka*, 1986.

Srinivasan, J., A simple thermodynamic model for seasonal variation of monsoon rainfall, *Curr. Sci. 80*, 73-77, 2001

Tegen, I., and I. Fung, Contribution to the atmospheric mineral aerosol load from land surface modification, *J. Geophys. Res.*, *100*, 18707-18726, 1995.

Torres, O., P. K. Bhartia, J. R. Herman, Z. Ahmad, and J. Gleason, Derivation of aerosol properties from satellite measurements of backscattered ultraviolet radiation: Theoretical basis, *J. Geophys. Res.*, *103*, 17099-17100, 1998.

Wen, S., and W. I. Rose, Retrieval of sizes and total masses of particles in volcanic clouds using AVHRR bands 4 and 5, *J. Geophys. Res.*, *99*, 5421-5431, 1994.